



## Optimization of the water vapor permeability of starch/alginate edible system reinforced with microcrystalline cellulose for the shelf-life extension of green capsicums



CrossMark

Hend E. Salama\*, Mahmoud G. Elsoholy, Mohamed S. Abdel Aziz, Gamal R. Saad

Chemistry Department, Faculty of Science, Cairo University, Giza, 12613, Egypt.

### Abstract

Water vapor permeability (WVP) is an important parameter for systems used in edible coatings of food. WVP should be optimized to a minimum value to control the passage of fluids between food and its environment. In this work, Box-Behnken design was applied to optimize the edible coating based on alginate, soluble starch and microcrystalline cellulose (MCC) to its minimum. The optimized theoretical value of WVP was 9.94 g mm/m<sup>2</sup> day kPa which was in agreement with the experimental obtained value. The molecular structure of the prepared edible coating films was verified using FTIR. MCC addition significantly improved the thermal and mechanical properties of the edible coating. Shelf-life studies on green capsicums coated with the optimized edible system showed great resistance to mass loss and spoilage. The prepared edible coating, based on the excellent obtained data, could be used potentially to extend the shelf-life of food.

**Keywords:** Edible coating; water vapor permeability; Box-Behnken design; alginate; microcrystalline cellulose.

### 1. Introduction

Edible films and coatings are thin layers of shielding materials that are used to extend the shelf-life of food [1-3]. Polysaccharides, proteins, and lipids have a variety of advantages in the preparation of edible coatings due to their biodegradability, edibility and biocompatibility [4-6]. Polysaccharides contain many functional groups which might be functionalized to interesting derivatives of improved properties [7-18]. Among biodegradable polysaccharides used as packaging, starch is commonly used as packaging due to its availability, ease of handling and generation from renewable resources. Starch consists primarily of linear and branched chains of glucose molecules, namely amylose and amylopectin, respectively [19]. Amylose, which is the linear fraction of starch, is responsible for the formation of coherent, relatively strong and free-standing films. Physical cross-linkages in the macromolecular network of starch are formed mainly by microcrystalline amylose and affect the mechanical properties of films [20]. Starch-based edible coatings exhibit excellent physical characteristics such as being transparent [21], odorless, tasteless [22], good barrier and mechanical properties [23]. Many researchers tried to improve the

properties of starch films of improved properties by blending them with other biopolymers, such as alginate [24], chitosan [25] and pullulan [5].

On the other hand, sodium alginate is another type of polysaccharide composing of *D*-mannuronic acid (M) and *L*-guluronic acids (G) units. It is water-soluble and non-toxic. Alginate has potential use in the edible film's preparation due to its unique colloidal and gel-forming properties in the presence of multivalent cations as Ca<sup>2+</sup>. Many reports described the application of alginate and its composites films in the field of edible coatings [4, 26]. Unfortunately, alginate suffers from some drawbacks like bad mechanical, barrier and antimicrobial properties, which limit its wide usage in technical applications [27]. Further improvements should be performed to overcome these problems including the incorporation of active materials like antimicrobials [26] and reinforcing nanofillers [28, 29].

Microcrystalline cellulose (MCC) is among the most commonly used cellulose derivatives in the food industry as a compatible reinforcing filler for biopolymers used in edible coatings. The incorporation of MCC into starch films appears particularly interesting due to the chemical similarities

\*Corresponding author Emails: [hend\\_ezzat2010@yahoo.com](mailto:hend_ezzat2010@yahoo.com), [hendezzat2010@cu.edu.eg](mailto:hendezzat2010@cu.edu.eg)

Receive Date: 07 March 2021, Revise Date: 25 March 2021, Accept Date: 05 April 2021

DOI: 10.21608/EJCHEM.2021.66683.3434

©2021 National Information and Documentation Center (NIDOC)

in their structure. This could lead to good compatibility between MCC and starch films which is very important to improve mechanical, thermal and barrier properties of the developed coatings [30].

Among the critical specifications of edible films is their barrier properties represented in the form of water vapor permeability (WVP) parameter. Edible films should have low WVP to keep food fresh and retards its spoilage. Generally, WVP is affected by many factors including the composition of the materials used in the preparations of edible coatings. These factors have to be optimized to get a sophisticated edible coating of the minimum value of WVP. Recently, response surface methodology (RSM) is applied to optimize and analyze complex reactions including many factors to a certain limit [1, 31].

Usually, the formulation of an edible system consisting of many different components is a complex process due to the difficulties in determining the best reaction conditions. This process became more difficult when the formulation is directed to design an edible system of a specific property. In the current work, starch, alginate and MCC were optimized using the Box-Behnken design to obtain edible films of the lowest WVP. The physical, thermal and mechanical properties of the prepared coating films were investigated and their application for the shelf-life extension of green capsicums was evaluated.

## 2. Experimental

### 2.1. Materials

Sodium alginate ( $M_w = 3 \times 10^5$  g/mol), soluble starch, microcrystalline cellulose (51  $\mu\text{m}$  mesh) and solvents were supplied from Sigma-Aldrich (Germany).

**Table 1.** Levels of the three used variables.

Variables (unit)	Factors	Levels		
		Low (-1)	Middle (0)	High (+1)
Alginate (g)	$x_1$	1	2	3
Starch (g)	$x_2$	1	2	3
MCC (wt%)	$x_3$	2	4	6

### 2.4. Characterization techniques

#### 2.4.1. FTIR

FTIR spectra were obtained using a Perkin-Elmer B25 spectrophotometer. 10 scans were recorded from 4000–400  $\text{cm}^{-1}$  with a resolution of 4  $\text{cm}^{-1}$ .

#### 2.4.2 XRD

XRD patterns were recorded using Philips Xpert MPD Pro with Cu-K $\alpha$  radiation source ( $\lambda = 1.54056$   $\text{\AA}$ ). The films were scanned during the  $2\theta$  range of 5°–35°.

#### 2.4.3. Thermogravimetric analysis (TGA)

TGA was measured using Shimadzu TGA-50 H Thermal Analyzer (Shimadzu, Tokyo, Japan). The

### 2.2. Preparation of alginate/starch/MCC films

A predetermined amount of alginate was dissolved in distilled water under stirring, then the prepared solution was added portionwise to another aqueous solution containing a certain amount of starch. MCC was dispersed in the least amount of distilled water, then the dispersion was added dropwise to the prepared alginate/starch solution with continuous stirring. The amounts of alginate, starch and MCC were determined according to the experimental matrix generated by Box-Behnken design (BBD) in Table 1. Glycerol was added in 40 wt% to the reaction mixture followed by stirring at room temperature for 2 h. The films were obtained by casting into Petri dishes followed by drying at 40°C for 24 h in a vacuum oven. After that, the unpeeled films were dipped in 45 mL of CaCl<sub>2</sub> and re-dried again in the oven for 2 h at 40°C. The dried films obtained were peeled off, washed with de-ionized water to remove the unreacted calcium chloride then stored at room temperature for evaluation [4].

### 2.3. BBD for alginate/starch/MCC edible films

The BBD was applied to investigate and optimize the reaction variables (alginate  $x_1$ , starch  $x_2$  and MCC  $x_3$ ) for the minimum WVP value. In this model, each variable was studied at three levels, low (-1), middle (0), and high (+1) as shown in Table 1. In this model, 15 experiments are required to study the three variables. Three replicates were performed at the center points (level 0) of the three variables to estimate the error. Table 2 illustrates the 15 runs including the experimental and theoretical values of WVP.

samples (4–5 mg) were heated from room temperature to 500 °C under N<sub>2</sub> gas (50 ml/min) with a heating rate of 10 °C min<sup>-1</sup>.

#### 2.4.4. Mechanical testing

Mechanical testing was conducted using the Zwick 1445 (Zwick GmbH, Germany) following the ASTM D882-2010 standard [32]. Five tests were conducted for each film, and the obtained parameters were averaged.

#### 2.4.5. WVP

ASTM E96-92 (1990) [33] was applied to determine WVP where a permeation cell containing

distilled water was sealed with the prepared films (100% RH; 2.337 kPa vapor pressure at 20 °C). The permeation cell was placed in a desiccator (0% RH, 0 kPa vapor pressure at 20 °C), and the mass loss was measured every 2 h over 24 h. WVP can be determined as follows:

$$\frac{w \cdot x}{A \cdot \Delta P} = (WVP) \cdot t$$

where  $x$  (in mm) is the film thickness,  $A$  ( $m^2$ ) is the permeation area,  $\Delta P$  (kPa) is water vapor partial pressure difference across films,  $t$  (day) is time and  $w$  (g) is the mass loss. Three independent measurements were conducted for each film, and the values of WVP were averaged.

#### 2.4.6. Shelf-life studies

Fresh green capsicums of approximate size without any defects were sterilized using 0.1 g/L of hypochlorite solution for 2 min then rinsed and dried. Capsicums were coated with a thin layer of films by dipping them in the film solution many times followed

by drying. The mass of capsicums was followed and recorded every two days for 13 days. The mass loss percentage was determined as follows:

$$\text{Mass loss (\%)} = \frac{100 \times (m_o - m_t)}{m_o}$$

where  $m_t$  is the final capsicum mass after each interval and  $m_o$  is the capsicum mass on day 1. Three fruits of approximate size were coated by the same film, and the obtained results were averaged for each film. Images of capsicums were captured during periodical time intervals to detect any spoilage on their surface.

#### 2.4.7. Statistical analysis

Statistical analysis by the analysis of variance (ANOVA) was carried by SPSS® 16. All experiments were carried out in three independent runs, and the measured parameters were averaged and expressed as the mean  $\pm$  standard error where each value is considered as a significant at  $p < 0.05$ .

**Table 2.** Box-Behnken design (BBD) runs with experimental and predicted WVP.

Run	Alginate (g)	Starch (g)	MCC (wt%)	Experimental WVP	Predicted WVP
1	3	3	4	20.30	20.03
2	1	2	2	19.20	19.34
3	2	2	4	17.20	17.20
4	1	3	4	16.40	15.85
5	2	2	4	17.20	17.20
6	2	1	6	12.10	11.69
7	3	2	2	23.20	23.06
8	2	2	4	17.20	17.20
9	2	1	2	20.10	19.69
10	2	3	2	22.20	22.61
11	2	3	6	14.40	14.81
12	1	1	4	13.00	13.28
13	1	2	6	11.30	11.44
14	3	1	4	16.00	16.55
15	3	2	6	15.30	15.16

### 3. Results and discussion

#### 3.1. BBD

BBD was used to optimize the three variables of the individual components used for the preparation of edible films to get the minimum WVP value. The quadratic equation for WVP ( $Y$ ) generated through BBD is generally expressed as:

$$Y = A_0 + A_1x_1 + A_2x_2 + A_3x_3 + A_{12}x_1x_2 + A_{13}x_1x_3 + A_{23}x_2x_3 + A_{11}x_1^2 + A_{22}x_2^2 + A_{33}x_3^2$$

(3)

where  $A_0$  is the intercept,  $x_1$  is the mass of alginate,  $x_2$  is the mass of starch,  $x_3$  is the percent of MCC and  $A_0$ – $A_{33}$  are the regression coefficients.

The quadratic equation for WVP generated by BBD in terms of the actual values is:

$$WVP = 18.0 + 2.86250x_1 + 2.61250x_2 - 2.85000x_3 + 0.225000x_1x_2 - 1.09 \times 10^{-16}x_1x_3 + 0.025000x_2x_3 - 0.362500x_1^2 - 0.412500x_2^2 + 0.103125x_3^2$$

(4)

The regression of the model equation can be improved through the elimination of the non-significant terms ( $p > 0.05$ ) depicted in Table 3 to be:

$$WVP = 18.0 + 2.86250x_1 + 2.61250x_2 - 2.85000x_3$$

(5)

**Table 3.** ANOVA analysis of WVP.

Source	Sum of Squares	df	Mean Square	F-value	p-value	Effect
<b>Model</b>	172.94	9	19.22	63.52	0.0001	Significant
$x_1$	27.75	1	27.75	91.74	0.0002	Significant
$x_2$	18.30	1	18.30	60.50	0.0006	Significant
$x_3$	124.82	1	124.82	412.63	< 0.0001	Significant
$x_1x_2$	0.2025	1	0.2025	0.6694	0.4505	Non-significant
$x_1x_3$	0.0000	1	0.0000	0.0000	1.0000	Non-significant
$x_2x_3$	0.0100	1	0.0100	0.0331	0.8629	Non-significant
$x_1^2$	0.4852	1	0.4852	1.60	0.2611	Non-significant
$x_2^2$	0.6283	1	0.6283	2.08	0.2091	Non-significant
$x_3^2$	0.6283	1	0.6283	2.08	0.2091	Non-significant
<b>Residual</b>	1.51	5	0.3025			
Lack of Fit	1.51	3	0.5042			
Pure Error	0.0000	2	0.0000			
<b>Cor Total</b>	174.45	14				
$R^2$	0.9913					
Adjusted $R^2$	0.9757					
Predicted $R^2$	0.8613					
Adeq precision	25.8867					

### 3.3.1. The adequacy of the proposed models

The validity of the proposed models must be verified to ensure the adequacy of the model to predict the WVP. The  $p$ -value parameter measures the significance of the proposed model where a  $p$ -value less than 0.05 confirms the significance of the model. A  $p$ -value of 0.0001 for WVP indicates the significance of the proposed model.

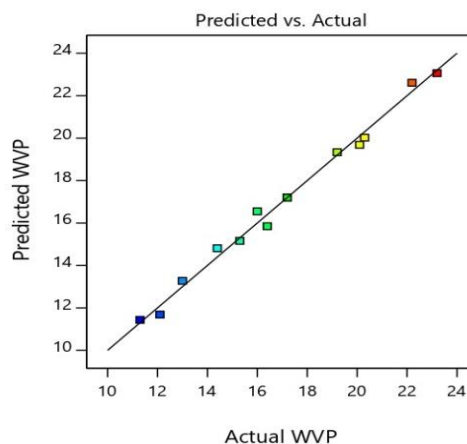
The  $F$ -value of 63.52 confirms that the proposed model is significant. The high predicted  $R^2$  of 0.86 confirms the reasonable fitness of the proposed model.

The adequate precision of any model is desired when its value  $> 4$ . The obtained value of 25.8867 ensures the adequacy of the proposed model. The adequacy of the proposed model can be also verified by comparing the predicted and measured values as seen in Fig. 1. As detected, both actual and predicted values of WVP are distributed along a straight line where they are very close to each other. This confirms the high agreement between both actual and predicted values and consequently the validity of the used model to represent WVP.

### 3.1.2. The combined effect of variables on WVP

Fig. 2a-c shows the combined effects of each two variables on WVP, while the third variable was kept constant at level 0. As depicted in Fig. 2a, the

WVP was increased upon either the increase in the content of alginate or starch. This is due to increasing the hydrophilic nature of both alginate and starch. As seen in Fig. 2b, WVP was decreased upon increasing the content of MCC due to increasing the crosslinking density resulted from the formation of hydrogen bonding between MCC and both alginate and starch. It is also observed the WVP was increased upon increasing the alginate content. From Fig. 2c, WVP was decreased either by increasing the MCC content or decreasing the starch content.

**Fig. 1.** Predicted vs. actual values for WVP.

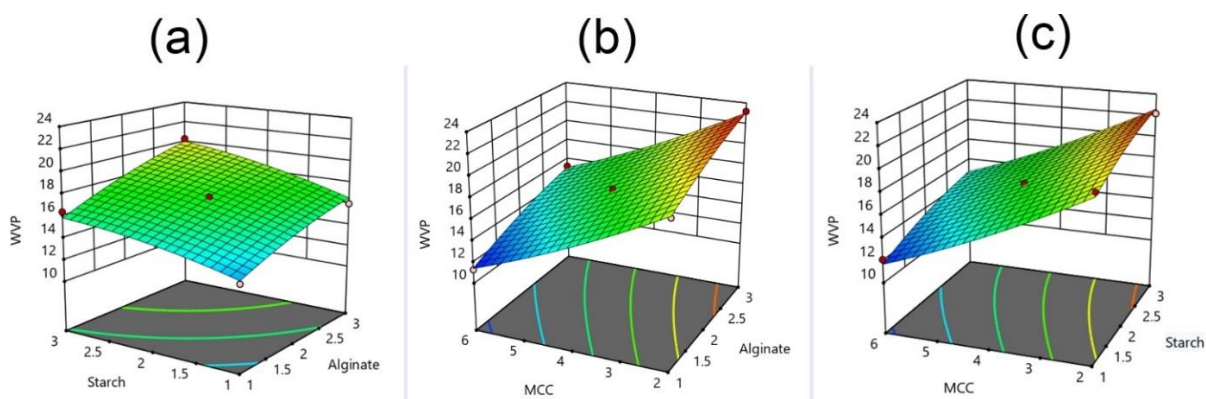


**Fig. 2.** 3D curves for the combined effects of (a) starch and alginate, (b) MCC and alginate, and (c) MCC and starch on WVP.

### 3.1.3. Optimization and validation

The optimized conditions generated by BBD of the film formulation for the minimized WVP are alginate = 1.00 g, starch = 1.04 g and MCC = 5.89 wt% (with respect to the total weight of alginate and starch) where the optimized theoretical value of WVP is 9.94 g mm/m<sup>2</sup> day kPa.

To check the validity of the proposed model, WVP was experimentally measured for a film prepared using the proposed optimized composition and found to be 10.01±0.23 g mm/m<sup>2</sup> day kPa, indicating that both measured and theoretical WVP are very close to each other which confirms the adequacy of the proposed model to describe the behavior of WVP. The film prepared using the optimal conditions was labeled here as O(Alg/St/MCC). Another film was prepared by using the optimal conditions of alginate and starch only without MCC for the sake of comparison, and this film was labeled as Alg/St.

### 3.2. FTIR

FTIR was performed to confirm the molecular structure of the prepared formulation and analyze the interactions between their alginate, starch, and MCC components.

FTIR spectra of the prepared films and their components are depicted in Fig. 3. Alginate showed a broad band around 3445 cm<sup>-1</sup> due to O-H stretching, while the asymmetric and symmetric stretching of carboxylate groups are observed at 1614 and 1420 cm<sup>-1</sup>, respectively [8, 34, 35].

The spectrum of starch revealed a characteristic broad band around 3431 cm<sup>-1</sup> due to the stretching vibration of -OH group. The broad bands that appeared during 3000-2800 cm<sup>-1</sup> are due to the C-H stretching. The bands that appeared within the range between 1050 cm<sup>-1</sup> and 940 cm<sup>-1</sup> are due to the deformation of C-OH while the band around 1150 cm<sup>-1</sup> is due to the C-O stretching vibration.

From the FTIR spectrum of Alg/St, some changes were observed compared with that of alginate

or starch. The two characteristic bands for the C-H asymmetric and symmetric stretching were shifted to a lower wavenumber compared with pure alginate. In addition, the band of the -OH stretching of the Alg/St system was broadened compared with their individual components. These changes may be due to the increase in the hydrogen bonding between alginate and starch resulting in good molecular compatibility.

For the spectrum of O(Alg/St/MCC), the incorporation of MCC didn't significantly change the profile spectrum of Alg/St due to the symmetry of its structure to both alginate and starch. However, one can notice the broadness of the -OH band was increased while the bands for the asymmetric and symmetric stretching of carboxylate groups were shifted to lower wavenumbers. This confirms the interactions between MCC with starch and alginate through hydrogen bonding.

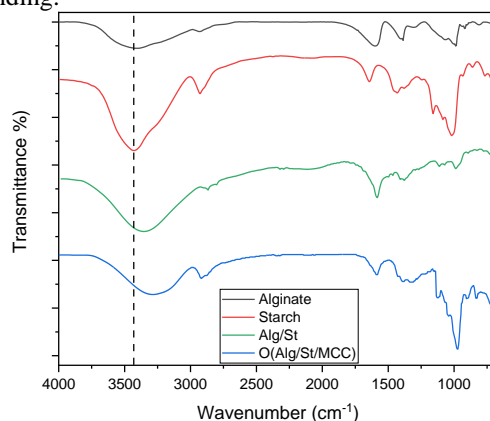


**Fig. 3.** FTIR spectra of alginate, starch, Alg/St and O(Alg/St/MCC).

### 3.3. XRD

The crystallinity of prepared films can be studied using XRD as shown in Fig. 4. The X-ray diffraction pattern of alginate showed a broad band at 2θ = 21.1° [4, 6, 8, 26] while that of starch showed characteristic peaks at 2θ = 15.2°, 16.9°, 18.2° and 23.2° [19]. MCC exhibited a small broad peak at 2θ = 15.3° and a large sharp peak at 2θ = 22.1°. However,

the XRD pattern of Alg/St showed a lower value of the degree of crystallinity, which is evidenced by the presence of a new broad peak at  $2\theta=20.9^\circ$  while the peaks of starch and alginate polymers were disappeared. Comparing O(Alg/St/MCC) with their pure constituents and Alg/St system, the XRD curve displayed a broader and less intense peak at  $2\theta=20.9^\circ$ , revealing the compatibility of MCC with alginate and starch polymers, and the formation of a film of more amorphous character [36].

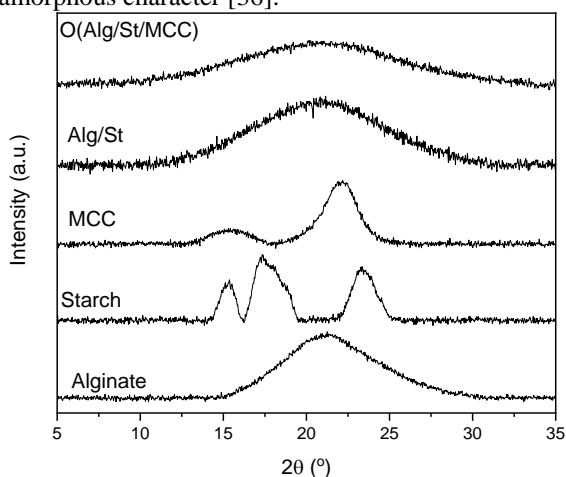


**Fig. 4.** XRD patterns of alginate, starch, MCC, Alg/St and O(Alg/St/MCC)

### 3.4. Thermal stability by TGA

Edible coatings have to be thermally stable within a wide range of temperatures to resist thermal decomposition during food storage. Fig. 5 depicts the TGA thermograms of Alg/St and O(Alg/St/MCC). For Alg/St, the first stage in mass loss is due to the evaporation of absorbed water. The second stage of about 15 % mass loss is due to the degradation of the main backbone of alginate and starch chains including dehydroxylation and decarboxylation. The third decomposition step of about 20 % mass loss due to the decomposition of the physically crosslinked structure. For the optimized film, O(Alg/St/MCC), a similar profile of thermogram to that of Alg/St was observed. However, the degradation steps were shifted to higher temperatures. In addition, the residual mass of O(Alg/St/MCC) was higher than that of Alg/St. This is due to the crosslinking reactions established due to the presence of MCC which somewhat resists the thermal decomposition and the residual of CaO generated from the use of  $\text{Ca}^{2+}$  as cross-linking agent, and thus higher thermal stability was attained. Thermal stability of the prepared films can be better viewed in terms of the integral procedure decomposition temperature (IPDT) [37] calculated as follows:

$$\text{IPDT} = A \cdot K(T_f - T_i) + T_i \quad (6)$$

The determination of  $A$ ,  $K$ ,  $T_f$  and  $T_i$  are explained in the supplementary data S1. A high IPDT value means better whole thermal stability. The calculated IPDT of Alg/St was 1044 while that of the optimized film O(Alg/St/MCC) was 1249. This confirms again that the presence of MCC in the optimized film enhanced its thermal stability.

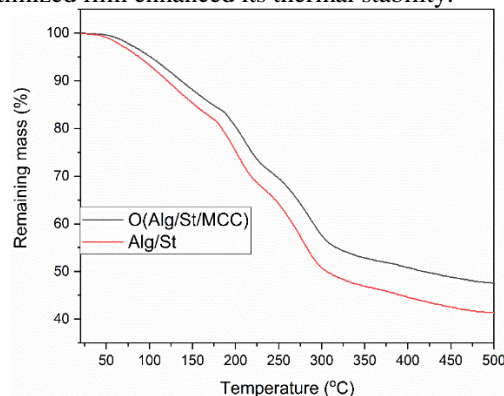


**Fig. 5.** TGA thermograms of Alg/St and O(Alg/St/MCC).

### 3.5. Mechanical properties

Edible coatings must have good mechanical properties to resist the stress during storage or the transportation of food. Fig. 6 depicts the mechanical properties of Alg/St and O(Alg/St/MCC). As seen, the tensile strength was increased from  $17.9 \pm 0.91$  MPa for Alg/St to  $19.8 \pm 0.99$  MPa for O(Alg/St/MCC). This was due to an increase in the interfacial interaction or/and extent of cross-linking between Alg and St matrices and MCC filler as a result of the chemical similarity (polysaccharide structure) of their constituents. On the other hand, the elongation at break was slightly decreased from 19 % for Alg/St to 17% for O(Alg/St/MCC) due to increasing the film stiffness.

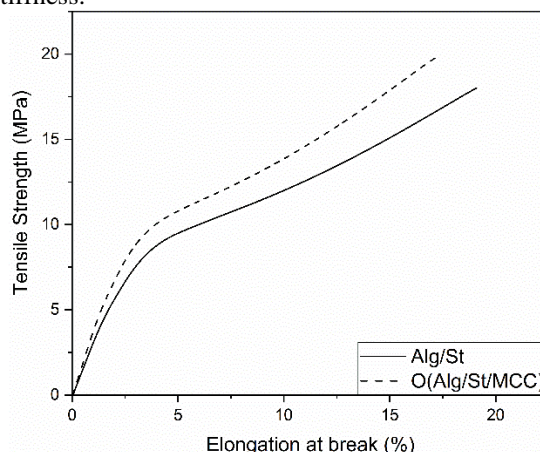


**Fig. 6.** Mechanical behavior of Alg/St and O(Alg/St/MCC).

### 3.6. Shelf-life studies

The shelf-life of green capsicums can be studied by observing any surface spoilage and following the mass loss of the coated and uncoated (control) capsicums during a storage period of 13 days.

Fig. 7, shows images of the investigated capsicums during the storage period along with the mass loss during this period. As can be seen in Fig. 7, the uncoated capsicum suffered from a high mass loss where about 45% of its mass was lost on the 13<sup>th</sup> day. On the other hand, the mass loss was significantly decreased when the capsicum was coated with the optimized edible system where the mass loss was only 6% on the 13<sup>th</sup> day. This significant resistance to mass loss is due to the excellent barrier properties of the prepared edible coating where WVP was optimized to its minimum using Box-Behnken design. The barrier properties are mainly due to hindering the passage of fluids from capsicums to their environment due to the high physical crosslinking density resulted from the hydrogen bonding and ionic interaction between the film components.

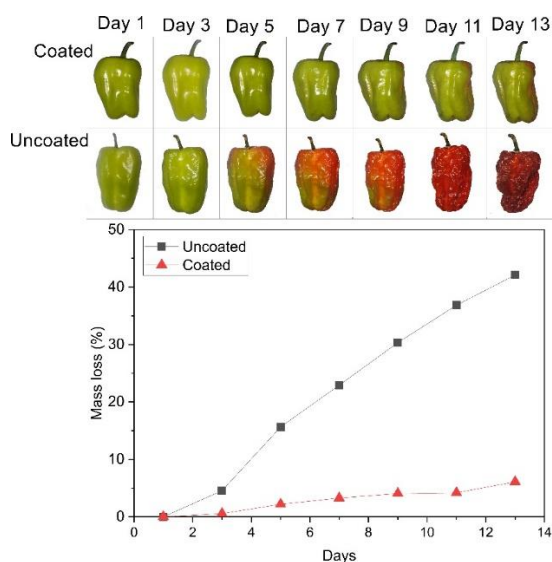


**Fig. 7.** Mass loss with time for the coated and uncoated capsicums with their images during the storage period.

#### 4. Conclusions

Box-Behnken design (BBD) was applied to optimize an edible coating system based on alginate, soluble starch and MCC as reinforcing filler to the minimized WVP. BBD proposed that WVP was reduced by increasing the content of MCC or decreasing the content of either alginate or starch. FTIR and XRD confirmed the compatibility between MCC with alginate and starch. The incorporation of MCC significantly enhanced the thermal stability of the films as mirrored from the IPDT value. The tensile strength was increased while the elongation at break was slightly decreased in the presence of MCC. The efficiency of the prepared edible coating system was examined in the extension of the shelf-life of green capsicums where significant resistance to spoilage and mass loss were obtained. The prepared edible coating systems exhibited improved physical

and chemical properties promoting them as potential candidates in food packaging industries.

#### References

- Salama H.E. and Abdel Aziz M.S., Optimized carboxymethyl cellulose and guanidylated chitosan enriched with titanium oxide nanoparticles of improved UV-barrier properties for the active packaging of green bell pepper. *International Journal of Biological Macromolecules*. **165**: 1187-1197 (2020)
- Salama H.E., Abdel Aziz M.S. and Sabaa M.W., Development of antibacterial carboxymethyl cellulose/chitosan biguanidine hydrochloride edible films activated with frankincense essential oil. *International Journal of Biological Macromolecules*. **139**: 1162-1167 (2019)
- Salama H.E., Abdel Aziz M.S. and Sabaa M.W., Novel biodegradable and antibacterial edible films based on alginate and chitosan biguanidine hydrochloride. *International Journal of Biological Macromolecules*. **116**: 443-450 (2018)
- Abdel Aziz M.S., Salama H.E. and Sabaa M.W., Biobased alginate/castor oil edible films for active food packaging. *LWT*. **96**: 455-460 (2018)
- Abdel Aziz M.S. and Salama H.E., Biocompatible and antimicrobial carboxymethyl xanthan/zinc physical hydrogels. *Polymer Bulletin*: (2021). <https://doi.org/10.1007/s00289-021-03668-z>
- Salama H.E. and Abdel Aziz M.S., Optimized alginate and Aloe vera gel edible coating reinforced with  $n\text{TiO}_2$  for the shelf-life extension of tomatoes. *International Journal of Biological Macromolecules*. **165**: 2693-2701 (2020)
- Fahmy Y., Fahmy T.Y., Mobarak F., El-Sakhawy M. and Fadl M., Agricultural residues (wastes) for manufacture of paper, board, and miscellaneous products: Background overview and future prospects. *International Journal of ChemTech Research*. **10**(2): 424-448 (2017)
- Salama H.E. and Abdel Aziz M.S., Development of active edible coating of alginate and aloe vera enriched with frankincense oil for retarding the senescence of green capsicums. *LWT*: 111341 (2021). <https://doi.org/10.1016/j.lwt.2021.111341>
- Saad G.R., Salama H.E., Mohamed N.A. and Sabaa M.W., Crystallization and thermal properties of biodegradable polyurethanes based on poly[(R)-3-hydroxybutyrate] and their composites with chitin whiskers. *Journal of Applied Polymer Science*. **131**(18): 9395-9407 (2014)

10. Salama H.E. and Abdel Aziz M.S., Development of Antibacterial Xanthan/Chitosan Biguanidine Hydrochloride Polyelectrolyte Complexes Decorated with Eco-friendly Prepared Silver Nanoparticles. *Nanoscience & Nanotechnology-Asia*. **10**: 1-10 (2020)
11. Salama H.E. and Abdel Aziz M.S., Novel biocompatible and antimicrobial supramolecular O-carboxymethyl chitosan biguanidine/zinc physical hydrogels. *International Journal of Biological Macromolecules*. **163**: 649-656 (2020)
12. Maher Y.A., Ali M.E.A., Salama H.E. and Sabaa M.W., Preparation, characterization and evaluation of chitosan biguanidine hydrochloride as a novel antiscalant during membrane desalination process. *Arabian Journal of Chemistry*. **13**(1): 2964-2981 (2020)
13. Abdel Aziz M.S., Salama H.E. and Saad G.R., Diglycidyl ether of bisphenol A/chitosan-graft-polyaniline composites with electromagnetic interference shielding properties: Synthesis, characterization, and curing kinetics. *Polymer Engineering and Science*. **59**(2): 372-381 (2019)
14. Salama H.E., Abdel Aziz M.S. and Saad G.R., Thermal properties, crystallization and antimicrobial activity of chitosan biguanidine grafted poly(3-hydroxybutyrate) containing silver nanoparticles. *International Journal of Biological Macromolecules*. **111**: 19-27 (2018)
15. Salama H.E., Saad G.R. and Sabaa M.W., Synthesis, characterization and antimicrobial activity of biguanidinylated chitosan-g-poly[(R)-3-hydroxybutyrate]. *International Journal of Biological Macromolecules*. **101**: 438-447 (2017)
16. Salama H.E., Saad G.R. and Sabaa M.W., Synthesis, characterization, and biological activity of cross-linked chitosan biguanidine loaded with silver nanoparticles. *Journal of Biomaterials Science, Polymer Edition*. **27**(18): 1880-1898 (2016)
17. Mohamed N.A., Salama H.E., Sabaa M.W. and Saad G.R., Synthesis and characterization of biodegradable copoly(ether-ester-urethane)s and their chitin whisker nanocomposites. *Journal of Thermal Analysis and Calorimetry*. **125**(1): 163-173 (2016)
18. Salama H.E., Saad G.R. and Sabaa M.W., Synthesis, characterization and biological activity of Schiff bases based on chitosan and arylpyrazole moiety. *International Journal of Biological Macromolecules*. **79**: 996-1003 (2015)
19. El-Ghany N.A.A., Abdel Aziz M.S., Abdel-Aziz M.M. and Mahmoud Z., Antimicrobial and swelling behaviors of novel biodegradable corn starch grafted/poly(4-acrylamidobenzoic acid) copolymers. *International Journal of Biological Macromolecules*. **134**: 912-920 (2019)
20. Stading M., Hermansson A.-M. and Gatenholm P., Structure, mechanical and barrier properties of amylose and amylopectin films. *Carbohydrate Polymers*. **36**(2-3): 217-224 (1998)
21. Lourdin D., Coignard L., Bizot H. and Colonna P., Influence of equilibrium relative humidity and plasticizer concentration on the water content and glass transition of starch materials. *Polymer*. **38**(21): 5401-5406 (1997)
22. Wolff I.A., Davis H., Cluskey J., Gundrum L. and Rist C.E., Preparation of films from amylose. *Industrial & Engineering Chemistry*. **43**(4): 915-919 (1951)
23. Garcia M.A., Martino M.N. and Zaritzky N.E., Lipid addition to improve barrier properties of edible starch- based films and coatings. *Journal of food science*. **65**(6): 941-944 (2000)
24. Wu Y., Weller C., Hamouz F., Cuppett S. and Schnepf M., Moisture loss and lipid oxidation for precooked ground- beef patties packaged in edible starch- alginate- based composite films. *Journal of food science*. **66**(3): 486-493 (2001)
25. Pinzon M.I., Garcia O.R. and Villa C.C., The influence of Aloe vera gel incorporation on the physicochemical and mechanical properties of banana starch- chitosan edible films. *Journal of the Science of Food and Agriculture*. **98**(11): 4042-4049 (2018)
26. Salama H.E., Abdel Aziz M.S. and Alsehli M., Carboxymethyl cellulose/sodium alginate/chitosan biguanidine hydrochloride ternary system for edible coatings. *International Journal of Biological Macromolecules*. **139**: 614-620 (2019)
27. Ruan C., Zhang Y., Wang J., Sun Y., Gao X., Xiong G. and Liang J., Preparation and antioxidant activity of sodium alginate and carboxymethyl cellulose edible films with epigallocatechin gallate. *International Journal of Biological Macromolecules*. **134**: 1038-1044 (2019)
28. Abdel Aziz M.S., Naguib H.F., Sherif S.M. and Saad G.R., Preparation and Characterization of Biodegradable Polyurethane Nanocomposites

- Based on Poly(3-hydroxybutyrate) and Poly(Butylene Adipate) Using Reactive Organoclay. *Polymer - Plastics Technology and Engineering*. **53**(16): 1671-1681 (2014)
29. Naguib H.F., Abdel Aziz M.S. and Saad G.R., Effect of Organo-Modified Montmorillonite on Thermal Properties of Bacterial Poly(3-hydroxybutyrate). *Polymer - Plastics Technology and Engineering*. **53**(1): 90-96 (2014)
  30. Rico M., Rodríguez-Llamazares S., Barral L., Bouza R. and Montero B., Processing and characterization of polyols plasticized-starch reinforced with microcrystalline cellulose. *Carbohydrate Polymers*. **149**: 83-93 (2016)
  31. Abdel Aziz M.S. and Salama H.E., Effect of vinyl montmorillonite on the physical, responsive and antimicrobial properties of the optimized polyacrylic acid/chitosan superabsorbent via Box-Behnken model. *International Journal of Biological Macromolecules*. **116**: 840-848 (2018)
  32. Philadelphia P.A.S.f.T.a.M., *ASTM D882-2010. Testing, A. S. f., & Materials: Standard test method for tensile properties of thin plastic sheeting*. 2010, ASTM International. p. 167–176.
  33. E96-00 A.S. *Standard test methods for water vapor transmission of materials. Annual book of ASTM standards*. 2000. ASTM Philadelphia.
  34. Angadi S.C., Manjeshwar L.S. and Aminabhavi T.M., Novel composite blend microbeads of sodium alginate coated with chitosan for controlled release of amoxicillin. *International Journal of Biological Macromolecules*. **51**(1): 45-55 (2012)
  35. Su R., Zhu X.-L., Fan D.-D., Mi Y., Yang C.-Y. and Jia X., Encapsulation of probiotic *Bifidobacterium longum* BIOMA 5920 with alginate–human-like collagen and evaluation of survival in simulated gastrointestinal conditions. *International Journal of Biological Macromolecules*. **49**(5): 979-984 (2011)
  36. Wang L., Lin L., Chen X., Tong C. and Pang J., Synthesis and characteristics of konjac glucomannan films incorporated with functionalized microcrystalline cellulose. *Colloids and Surfaces A: Physicochemical and Engineering Aspects*. **563**: 237-245 (2019)
  37. Doyle C., Estimating thermal stability of experimental polymers by empirical thermogravimetric analysis. *Analytical Chemistry*. **33**(1): 77-79 (1961)